JOURNAL OF SOLID STATE CHEMISTRY 12, 362–369 (1975)

Concentration Dependence of Superconductivity in Rubidium Tungsten Bronzes*

DAVID R. WANLASS AND M. J. SIENKO

Baker Laboratory of Chemistry, Cornell University, Ithaca, New York 14850

Received July 11, 1974

Rubidium tungsten bronzes of composition Rb_xWO_3 ($0.20 < x < 0.33$) have been prepared in well-defined crystalline form and examined for superconductivity by flux-expulsion techniques. An unusual double maximum with peak values in the critical temperature of 4.35°K at $x = 0.20$ and 2.90°K at $x = 0.30$ is observed. One possible explanation would be enhanced electron–phonon coupling associated with ordering of rubidium occupancy in the hexagonal tunnels. The effect of acid etching was also examined; it was concluded that an observed increase in critical temperature is not due to hydrogen replacement for rubidium as was postulated. Critical magnetic field studies indicate type II behavior consistent with the Abrikosov–Ginzburg equation.

Introduction

Sweedler's discovery of superconductivity in tungsten bronzes (*1*) and subsequent finding by Remeika et al. (*2*) that the critical temperature can be increased by acid etching suggests use of this system to study the effect of composition on superconductivity in nonstoichiometric materials. The tungsten bronzes are compounds of composition M_xWO_3 where M atoms occupy interstitial sites in a modified WO_3 matrix and donate their valence electrons to the conduction band of the host material. The BCS theory (*3*), through an exponential dependence on the density of states at the Fermi level, would predict a monotonic dependence of critical temperature on carrier electron density and hence on rubidium content.

The metallic nature of the alkali tungsten bronzes has been well documented (*4*). Except at low values of x, where behavior is semiconducting, single-crystal resistivity studies, Hall measurement, thermoelectric power, magnetic susceptibility and NMR observations support a model in which the alkali atom has transferred its s valence electron to the empty $W5dt_{2g}$–$O2p\pi$ conduction band of the WO_3 network. For the specific case of rubidium tungsten bronzes, the structure is hexagonal (space group $D_{6h}^3 - C6/mcm$) in the range $0.20 < x < 0.33$. Corner-sharing WO_6 octahedra are linked into three-membered and six-membered rings so as to form channels parallel to the c axis; the rubidium ions are distributed in these channels statistically over the two occupancy sites per unit cell. Full occupation of both sites corresponds to $x = 0.33$; the precise lower limit at which the structure ceases to be hexagonal is not known.

In his investigation of the superconductivity of Rb_xWO_3, Sweedler (*5*) found a critical temperature of approximately 2.0°K for $x \approx 0.30$. The critical temperature varied somewhat from sample to sample and could be increased to as much as 7.7°K by leaching out Rb or by diffusing Rb out of the sample by heating it with WO_3. Annealing of treated samples in a vacuum reduced the transition temperature

---

* This research was sponsored by the Air Force Office of Scientific Research (AFSC) under Grant No. 74-2583 and was supported in part by the National Science Foundation and Materials Science Center at Cornell University. This report is based in part on the Ph.D. thesis of David Wanlass.

to approximately the value before treatment, and cold working reduced the amount of superconducting material by about 80%. Although there was clear implication that the superconducting critical temperature could be increased by decrease in the rubidium concentration, the exact form of the composition dependence was not established. Neither the rubidium content nor its range of inhomogeneity was clearly defined. Because other superconductivity work on potassium tungsten bronzes suffered equally from imprecise specification of metal content, e.g., $0.27 < x < 0.31$, this work was undertaken to establish the composition dependence of superconductivity in Rb_xWO_3. A further motivation for the investigation was that the apparent T_c vs x dependence appeared to conflict with BCS theory. Unless the band shape in Rb_xWO_3 is highly unusual, increasing x should move the Fermi level to a higher density of states, which according to BCS should mean higher T_c, just the opposite of which appeared to be the case. As a final incentive, there were no critical field data for tungsten bronzes, and it was believed useful to establish such information in order to make comparison with standard superconductivity equations.

Experimental

Preparation of Samples

Crystals of Rb_xWO_3 were prepared by a thermal vapor growth technique, starting with Rb_2WO_4, WO_3, and W as indicated in the following equation:

$$x/2\,Rb_2WO_4 + ((3-2x)/3)\,WO_3 + x/6\,W \rightarrow Rb_xWO_3.$$

The reactants were ground together in an agate mortar under a nitrogen atmosphere, evacuated in a quartz tube overnight at 140°C, and then sealed at about 10^{-5} Torr. Sample tubes were heated at 1060–1070°C for varying periods of time, depending on the size of crystals desired. After five days, crystals had grown to several mm in length. In all cases they were well-formed blue-black hexagonal prisms with extremely smooth mirror faces. Temperature control was very critical; temperatures below 1060°C resulted in no visible crystallinity, whereas temperatures above 1075°C resulted in attack on the quartz. Starting materials were Johnson–Matthey Specpure WO_3, Atomergic 99.95% W, and Rb_2WO_4 that was prepared from fusion at 940°C for 24 hr of Atomergic 99.9% Rb_2CO_3 and Johnson–Matthey Specpure WO_3.

Sample Analyses

Rubidium contents were determined by neutron activation analysis by the analytical facility of the Cornell Materials Science Center. Table I summarizes the data; the values of x are believed to be precise to 1% of the figures quoted. X-ray powder diffraction patterns were obtained for all samples using a General Electric XRD-5 diffractometer with Ni-filtered Cu$K\alpha$ radiation and W powder as internal standard. All the Rb_xWO_3 samples were found to be single phase and of hexagonal symmetry, having cell parameters as indicated in Table I. The probable error in the X-ray parameters is ±0.005 Å.

Magnetic Susceptibility

The magnetic susceptibilities were determined for four samples, using the Faraday technique and equipment which has been described elsewhere (*6*). Samples were measured as fine crystalline powders (50–400 mesh) taken directly from the reaction tubes without any grinding or other treatment. Table II shows the results. These are expressed as χ_M, the observed susceptibility per mole of

TABLE I

ANALYSES OF RUBIDIUM TUNGSTEN BRONZES

Sample (nominal composition)	% Rb (by analysis)	x in Rb_xWO_3 (by analysis)	a_0 (Å)	c_0 (Å)
$Rb_{0.20}WO_3$	6.81	0.200	7.40	7.53
$Rb_{0.23}WO_3$	7.90	0.233	7.40	7.53
$Rb_{0.26}WO_3$	8.88	0.264	7.395	7.54
$Rb_{0.28}WO_3$	9.33	0.279	7.395	7.55
$Rb_{0.29}WO_3$	9.61	0.288	7.38	7.55
$Rb_{0.30}WO_3$	10.00	0.301	7.38	7.56
$Rb_{0.32}WO_3$	10.14	0.305	7.38	7.56
$Rb_{0.33}WO_3$	10.83	0.329	7.38	7.57

TABLE II

MAGNETIC SUSCEPTIBILITIES OF RUBIDIUM TUNGSTEN BRONZES

Sample (Nominal composition)	$\chi_M \times 10^6$ (emu per mole)	$\kappa \times 10^6$ (emu per cm^3)	m^*/m_0
$Rb_{0.20}WO_3$	−10.5	0.20	0.96
$Rb_{0.26}WO_3$	−13.2	0.16	0.84
$Rb_{0.30}WO_3$	−10.3	0.27	1.03
$Rb_{0.33}WO_3$	−11.7	0.25	0.96

Rb_xWO_3; κ, the derived electronic susceptibility per cm^3 after diamagnetic corrections have been subtracted; and m^*, the apparent effective mass of the electrons assuming one free carrier per Rb and Pauli–Peierls-type susceptibility. All values shown are for room temperature (25°C). Measurements were also performed from 1.5 to 298°K on two other samples, $Rb_{0.28}WO_3$ and $Rb_{0.30}WO_3$. Susceptibility values were temperature-independent down to 77°K with a slight decrease in diamagnetism below that. Near 20°K and lower, a very small field dependence was noted. The motivation for carrying out the temperature studies was to test the hypothesis that failure to observe superconductivity in $Rb_{0.28}WO_3$ down to 1.2°K (see below) may have been due to trapping out of carriers to form localized paramagnetic centers that would have destroyed the superconductivity. No such paramagnetism was observed. In fact, at 1.5°K, the molar susceptibility of $Rb_{0.28}WO_3$ and $Rb_{0.30}WO_3$ were identical within the limits of error.

Superconductivity Measurements

Onset of superconductivity was measured by flux expulsion (Meissner effect). The output emf of a secondary coil wound around a quartz tube containing the tungsten bronze sample was observed while an ac voltage was impressed across a coaxial primary coil. The output signal was monitored with a PAR Model HR-8 lock-in amplifier. Temperature was measured simultaneously with a CryoCal germanium resistance thermometer that had been calibrated over the range 1.5–100°K. For determining the percent volume that becomes superconducting, the filling factor of the coil was calibrated with tantalum, which becomes superconducting at 4.5°K. Lock-in amplifier frequencies were 400 Hz for powders and 4000 Hz for single crystals.

Critical magnetic fields for disappearance of the superconductivity at various temperatures were measured by means of a solenoid that fitted over the tail of the outer dewar. The solenoid was calibrated with a specially wound precision test coil; the maximum magnetic field obtainable was 750 G. The earth's magnetic field was not compensated, since the materials of interest in this work had relatively high critical fields. It was observed that the rubidium tungsten bronzes showed type II behavior, i.e., transition from superconducting to normal state occurred not at a single value of the field but over a range of field values. The first penetration of flux occurs at a critical field H_{c1} lower than the thermodynamic critical field H_c, and penetration is complete at a higher critical field H_{c2}. Details of the measuring technique are given elsewhere (*7*). Table III gives the results for the superconductivity parameters. Sample designations are by nominal compositions as presented in Table I. The critical temperature is T_c, as defined by the midpoint of the inflection in the voltage/temperature curve. The width of the transition is ΔT_c, as defined by the voltage/temperature curve for the temperature interval required to go from the baseline coil voltage in the superconducting state to a constant coil voltage in the normal state. $H_{c2}(0)$, the upper critical field at zero temperature, was determined by extrapolation, assuming as noted below that the Abrikosov–Ginzburg equation gives the best fit to the data. Figure 1, which is for $Rb_{0.32}WO_3$

TABLE III

SUPERCONDUCTIVITY PARAMETERS OF RUBIDIUM TUNGSTEN BRONZES

Sample (Nominal composition)	T_c(°K)	ΔT_c(°K)	Superconducting volume (%)	$H_{c2}(0)$ (G)
$Rb_{0.33}WO_3$	2.15	0.12	100	643
$Rb_{0.33}WO_3$ (Single crystal)	2.15	0.025		645
$Rb_{0.32}WO_3$	2.37	0.11	100	925
$Rb_{0.30}WO_3$	2.80	0.08	100	1290
$Rb_{0.30}WO_3$ (Single crystal)	2.90	0.03		1039
$Rb_{0.29}WO_3$	2.30	0.40	100	950
$Rb_{0.28}WO_3$	<1.20			
$Rb_{0.26}WO_3$	<1.20			
$Rb_{0.23}WO_3$	~1.3	>0.1	2% from 1.3 to 1.2°	
$Rb_{0.20}WO_3$	4.35	0.30	67	

powder, gives a typical curve for the observed H_{c2} vs temperature dependence. The dots and bracketed interval are experimental points. The solid and dashed lines are least-squares computer curves generated from the experimental points and Abrikosov–Ginzburg or Gor'kov equations, respectively. Figure 2, which is for a single crystal of $Rb_{0.30}WO_3$, gives also a typical curve for the observed H_{c1} vs temperature dependence. With the technique used it was not possible to determine precise values of H_{c1} for powders, since for powder samples the superconducting baseline was slightly dependent on temperature. Anisotropy in H_{c2} and H_{c1} was looked for in the single crystal of $Rb_{0.30}WO_3$ by orienting

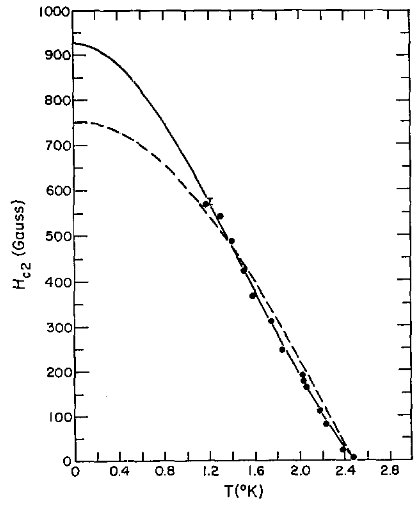

FIG. 1. Upper critical field H_{c2} vs temperature for $Rb_{0.32}WO_3$ powder. The solid and dashed lines represent Abrikosov–Ginzburg and Gor'kov equations, respectively.

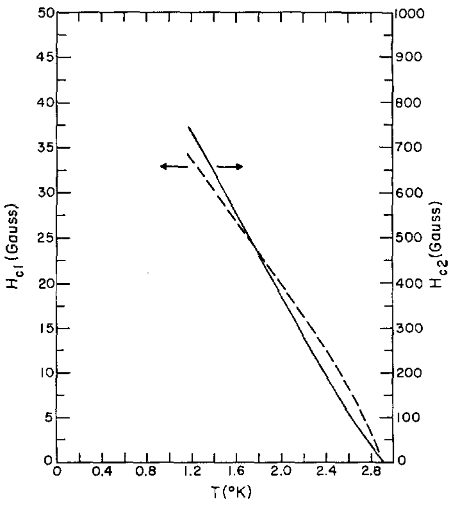

FIG. 2. H_{c1} and H_{c2} vs temperature for a single crystal of $Rb_{0.30}WO_3$. H_{c1} is the dashed curve for which the scale is on the left; H_{c2} is the solid curve; scale on the right.

the crystal so its c-axis would be parallel or perpendicular to the field, but no difference was observed.

Acid Etching

In an attempt to understand the discovery by Remeika et al. (*2*) that heating in a mineral acid could raise the superconducting transition temperatures of Rb_xWO_3, a number of different samples were acid etched under various conditions. Table IV summarizes the findings and compares the results with those obtained on a nonetched sample in which reduction of rubidium concentration was attempted by simple heating of a WO_3–Rb_xWO_3 mixture. As indicated by a change in color from dark-blue to grey, surface oxidation of the bronze probably occurs when it is acid etched by open heating. This is also indicated by reduction in the percent volume that goes superconducting. As can be seen from Table IV, acid-etched samples show superconductivity at higher temperatures and the transition is spread out from the original T_c over intervals on the order of degrees rather than tenths of a degree as before etching. Nuclear magnetic-resonance experiments designed to look for hydrogen diffused from the acid into the Rb_xWO_3 matrix, possibly in replacement for rubidium, were unsuccessful. Even so, any hypothesis that hydrogen entry into the bronze can be responsible for the observed rise in critical temperature can be rejected because, as shown by the bottom entry in Table IV, acid etching is not needed to produce the effect. For the last sample of Table IV, a mixture of WO_3 and $Rb_{0.30}WO_3$, put together without grinding so as to avoid cold working, was heated at 1000°C so a reduction of rubidium content could be achieved by diffusion of rubidium from the bronze to WO_3. The enhanced spread in critical temperature to a higher temperature was similar to that observed on acid etching.

Discussion

As given in Table III, the critical temperatures for well-defined homogeneous specimens of Rb_xWO_3 show, as a function of rubidium concentration, two regions of relatively high T_c separated by a trough. There appears to be a clear maximum, $T_c = 2.90°K$, at $x = 0.30$ in the range $0.28 < x < 0.33$ and another higher value of T_c, 4.35°K, at $x = 0.20$. Still higher values of T_c might be anticipated for x less than 0.20 on the basis of Sweedler's observation that etching raises T_c to as high as 7.7°K (*5*).

The observed double peak in T_c is rather surprising. The BCS theory gives

$$T_c = 1.14\,\theta \exp\left[-1/D(\varepsilon_F)\,V_{BCS}\right]$$

where θ is the Debye temperature, $D(\varepsilon_F)$ is the density of states at the Fermi level, and V_{BCS} is the phonon-mediated electron–

TABLE IV

INFLUENCE OF VARIOUS TREATMENTS ON SUPERCONDUCTING PARAMETERS OF Rb_xWO_3

Sample	Treatment	T_c(°K) Before	T_c(°K) After
$Rb_{0.28}WO_3$	Powder (230–400 mesh), etched in conc H_2SO_4 at 115°C, 24 hr in closed weighing bottle	<1.2	<1.2–3
$Rb_{0.30}WO_3$	Powder (325–400 mesh), etched in 50% H_2SO_4 at 230°C, 12 hr in open beaker	~2.7–2.87	~2.7–3.7
$Rb_{0.32}WO_3$	Powder (230 mesh), etched in 99.5% H_2SO_4 at 115°C, 26 hr in closed weighing bottle (N_2 atmosphere).	~2.2–2.47	~2.2–5.3
$Rb_{0.30}WO_3$	Powder (230–325 mesh) 5:1 M ratio WO_3: $Rb_{0.30}WO_3$ heated at 1000°C for 24 hr in evacuated quartz tube	~2.7–2.87	~2.7–4.6

sample showed a T_c of 2.1°K by both ac inductance and heat-capacity measurements, the etched sample showed a T_c of 3–5°K by mutual inductance and only a single peak at 2.1°K in the heat capacity.

For one of their acid-etched samples Remeika *et al.* (*2*) reported a smaller c_0 lattice parameter and a higher T_c than those found for $Rb_{0.20}WO_3$ in this work. Also Sweedler (*5*) reported T_c as high as 7.7°K. It may be that acid etching is able to produce a metastable hexagonal bronze with $x < 0.20$. King's finding (*8*) that a sample etched for a week at 100°C gave an enhanced transition temperature over the entire volume suggests that low-temperature etching might be a useful synthesis route to higher T_c materials. Phonon spectrum studies by inelastic neutron scattering of such low-x bronzes as well as of a series of bronzes of varying x would be most desirable.

References

1. A. R. Sweedler, C. J. Raub, and B. T. Matthias, *Phys. Rev. Letters* **15**, 108 (1965).
2. J. P. Remeika, T. H. Geballe, B. T. Matthias, A. S. Cooper, G. W. Hull, and E. M. Kelly, *Phys. Letters* **24A**, 565 (1967).
3. J. Bardeen, L. N. Cooper, and J. R. Schrieffer, *Phys. Rev.* **106**, 162 (1957); **108**, 1175 (1957).
4. For reviews on tungsten bronzes see M. J. Sienko, *Adv. Chem. Ser.* **39**, 224 (1963); P. G. Dickens and M. S. Whittingham, *Quart. Rev.* **22**, 30 (1968).
5. A. R. Sweedler, Ph.D. thesis, Stanford University, 1969.
6. J. E. Young, Jr., Ph.D. thesis, Cornell University, 1971.
7. D. R. Wanlass, Ph.D. thesis, Cornell University, 1973.
8. C. N. King, Ph.D. thesis, Stanford University, 1972.
9. C. S. Koonce, Marvin L. Cohen, J. F. Schooley, W. R. Hosler, and E. R. Pfeiffer, *Phys. Rev.* **163**, 380 (1967).
10. J. K. Hulm, C. K. Jones, R. A. Hein, and J. W. Gibson, *J. Low Temp. Phys.* **7**, 291 (1972).
11. See the excellent review article by J. K. Hulm, M. Ashkin, D. W. Deis, and C. K. Jones, *In* "Progress in Low Temperature Physics," (C. J. Gorter, Ed.), Vol. 6, pp. 205–242. American Elsevier, New York, 1970.
12. M. J. Sienko and S. M. Morehouse, *Inorg. Chem.* **2**, 485 (1963).
13. H. R. Shanks, *Solid State Comm.* (in press).
14. V. L. Ginzburg and L. D. Landau, *Zhur. Eksperimen. i Teor. Fiz.* **20**, 1064 (1950).
15. A. A. Abrikosov, *Zhur. Eksperim. i Teor. Fiz.* **32** 1442 (1957); V. L. Ginzburg, *idem* **30**, 593 (1956).
16. L. P. Gor'kov, *Zhur. Eksperim. i Teor. Fiz.* **37** 835, 1407 (1959).
17. J. L. Harden and V. Arp, *Cryogenics* **4**, 105 (1963).
18. A. J. Bevolo, H. R. Shanks, P. H. Sidles, and G. C. Danielson, *Phys. Rev. B* **9**, 3220 (1974).